

Structural Basis of X-Ray-Induced Transient Photobleaching in a Photoactivatable Green Fluorescent Protein

Virgile Adam,[†] Philippe Carpentier,[‡] Sebastien Violot,[§] Mickaël Lelimosin,[‡] Claudine Darnault,[‡] G. Ulrich Nienhaus,^{||,⊥} and Dominique Bourgeois^{*,‡}

European Synchrotron Radiation Facility, 6 rue Jules Horowitz, BP 220, 38043 Grenoble Cedex, France, IBS, Institut de Biologie Structurale Jean-Pierre Ebel, CEA, CNRS, Université Joseph Fourier, 41 rue Jules Horowitz, 38027 Grenoble, France, Laboratoire de Physiologie Cellulaire Végétale, Institut de Recherches en Technologie et Sciences pour le Vivant, CEA, CNRS, INRA, Université Joseph Fourier, 17 rue des Martyrs, F-38054 Grenoble, France, Institute of Applied Physics and Center for Functional Nanostructures (CFN), Karlsruhe Institute of Technology, 76128 Karlsruhe, Germany, and Department of Physics, University of Illinois at Urbana–Champaign, Urbana, Illinois 61801

Received August 28, 2009; E-mail: dominique.bourgeois@ibs.fr

Fluorescent proteins (FPs) are invaluable fluorescent markers in cell biology. Naturally occurring FPs have been optimized to emit bright fluorescence over a wide spectral range, and photoactivatable FPs have recently been developed that enable protein tracking¹ and play a crucial role in super-resolution microscopy.² Upon illumination, all FPs undergo transient stochastic switching events to nonfluorescent dark states, a phenomenon known as “blinking”.³ They eventually convert to a permanent off state, which is known as “bleaching”. Typically, the 4-(*p*-hydroxybenzylidene)-5-imidazolone chromophore bleaches because of intersystem crossing to the triplet state or excursions to protonated, isomerized, or radical states and emits 10⁴–10⁵ photons before falling victim to irreversible photodestruction. Although blinking and bleaching can be exploited in certain applications,^{4–7} they are generally considered as major nuisances, notably in single-molecule and time-resolved studies, and they limit the achievable resolution in several nanoscopy schemes.

Contrary to organic dyes^{8–12} or quantum dots,¹³ the details of the molecular mechanisms underlying the transient or permanent loss of fluorescence in FPs have remained largely unexplored, and the development of variants with superior photostability has followed empirical approaches.¹⁴ In organic dyes, electron-transfer reactions have been identified in the formation of transient dark radical states, which constitute important pathways for photobleaching.^{8–12} Radical chemistry can also occur in FPs, for example through the Kolbe^{15,16} or oxidative “redding”¹⁷ mechanisms. The short-lived nature of radical states in FPs, however, has prevented a structural characterization.

Here we have used X-ray radiolysis as a source of electrons and holes to generate a transient dark state in the photoactivatable fluorescent protein IrisFP,¹⁸ a variant of the fluorescent protein EosFP from *Lobophyllia hemprichii*.¹⁹ We noticed that the fluorescence emission of IrisFP crystals decays very rapidly under a synchrotron X-ray beam, even at 100 K (Figure 1a). This decay occurs at an X-ray dose much lower than that needed to collect a complete diffraction data set (typically 0.5–1.0 MGy) and is mostly reversible, with only a small irreversible component (Figure 1a, inset). The corresponding absorbance decay is composed of a rapid phase followed by a slower phase, is less pronounced at comparable

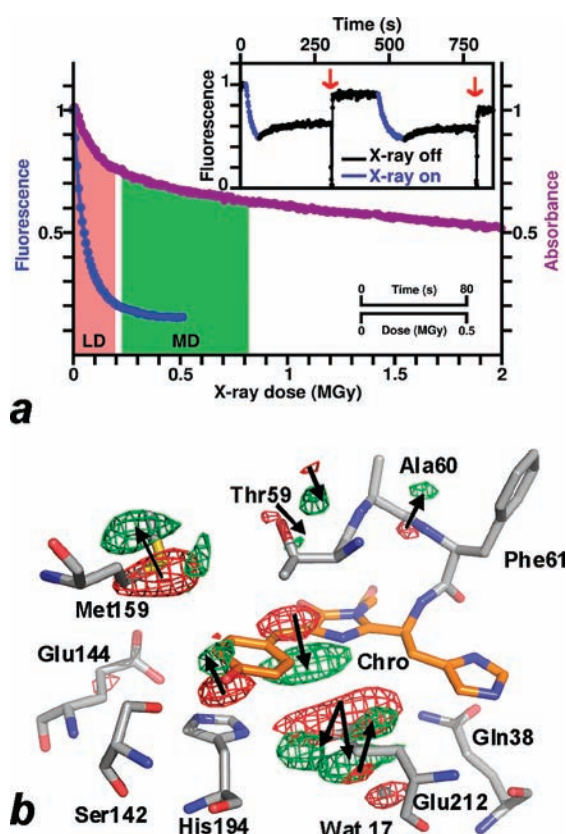


Figure 1. Reversible bleaching of IrisFP in crystallo induced by X-rays at 100 K. (a) Fluorescence (blue) and absorbance (purple) decays due to X-ray irradiation. The doses used for the two composite data sets [low dose (LD) and moderate dose (MD)] are indicated (red and green shading). The inset shows the reversibility of the fluorescence decay. Partial recovery (black) occurs at 100 K, whereas almost complete recovery is rapidly induced by short excursions to room temperature (red arrows at 300 and 780 s). The process can be repeated multiple times. (b) Experimental difference electron density map (red, -9.5σ ; green, $+9.5\sigma$) between the LD and MD data sets, overlaid on a model of IrisFP (PDB entry 2VVH). The difference map averaged over the four IrisFP monomers in the crystal asymmetric unit is shown (see the SI). The chromophore is displayed in orange and neighboring residues in gray. Arg66, in contact with the chromophore, has been omitted for clarity. Arrows indicate structural motions.

[†] European Synchrotron Radiation Facility.

[‡] Institut de Biologie Structurale Jean-Pierre Ebel.

[§] Institut de Recherches en Technologie et Sciences pour le Vivant.

^{||} Karlsruhe Institute of Technology.

[⊥] University of Illinois at Urbana–Champaign.

doses, and is also partly reversible [Figure 1a and Figure S1 in the Supporting Information (SI)].

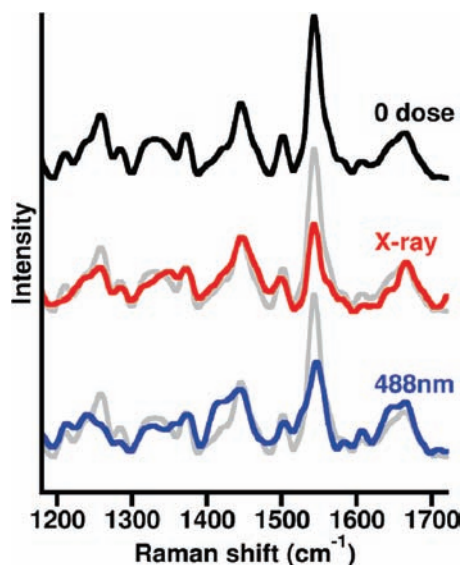


Figure 2. In crystallo Raman spectra of IrisFP. Spectra collected at 100 K are shown before (black and gray lines) and after X-ray irradiation (0.9 MGy; red line), and after 488 nm illumination (26 min at 1.2 kW/cm²; blue line).

To obtain a structural view of these transient spectroscopic changes, we collected composite X-ray diffraction data sets (see the SI)²⁰ in order to reconstruct two complete data sets that correspond to the beginning (median dose ~ 0.1 MGy) and end (~ 0.5 MGy) of the fast absorbance decay phase (Figure 1 and Table S1 in the SI). The difference electron density map between the two data sets reveals structural changes localized on the chromophore and its immediate environment (Figure 1b). Pairs of negative and positive difference density features show a downward motion of the chromophore's bridging methylene moiety and an upward motion of the benzylidene phenolate oxygen, resulting in a loss of planarity of the chromophore. The motion of the methylene bridge induces a displacement of Glu212 [Glu222 in green fluorescent protein (GFP)] that explores two conformations, with the carboxylate group H-bonded to either His194 or Gln38. The motion of the chromophore phenolate oxygen is accompanied by a shift of the Met159 side chain that is clearly visible because of the heavy sulfur atom. Other structural changes typically observed upon intense X-ray exposure of protein crystals are not visible at the doses employed here (Figure S2 in the SI).

In crystallo Raman spectra of IrisFP collected before and immediately after exposure to a moderate X-ray dose (0.9 MGy) reveal band modifications that are consistent with the observed structural changes (Figure 2; also see the SI). Notably, the band at 1545 cm⁻¹, which is the most strongly resonance-enhanced band in GFP,²¹ is significantly reduced. This band has been assigned to a mode that combines stretching of the C_α=C₅ exocyclic double bond (the methylene bridge; Scheme S1 in the SI) and deformation of the imidazolinone moiety of the anionic chromophore.²² A decrease of the 1545 cm⁻¹ band is consistent with a loss of the double-bond character of the methylene bridge, as suggested by the structural data. The 1545 cm⁻¹ band is probably converted to a lower-frequency band that cannot be identified in our spectra because it is weak and nonresonant. No other Raman band seems much altered, suggesting that the chromophore does not change its protonation state and that its phenol moiety remains chemically intact (Figure S3).²³ Altogether, the diffraction, UV-vis absorbance, and Raman data indicate that the C_α=C₅ π bond is reversibly altered

upon mild X-ray exposure, transiently disrupting the conjugated π-electron system.

Electron difference density maps obtained from data sets collected at moderate and much higher (~ 20 MGy) X-ray doses, mostly representative of structural changes associated with the slow absorbance decay phase, show a tilted chromophore and a clear decarboxylation of Glu212 (Figure S4), indicative of a permanently bleached state.

Because the reversible loss of color in the crystal is achieved with a number of absorbed X-ray photons orders of magnitude smaller than the number of diffracting protein molecules (see the SI), dark-state formation must result from a secondary radiation damage process.²⁴ As reactive oxygen species and solvated electrons produced by solvent radiolysis essentially do not diffuse at 100 K, electrons and holes migrating to the chromophore are most likely involved, resulting in protein radical states that eventually lead to permanent photodestruction. The fluorescence decay kinetics is probably accelerated by quenching effects attributable to absorbing radiolysis products (e.g., solvated electrons).²⁵ Thus, chemically intact chromophores may quickly lose their ability to fluoresce. The absorbance decay, in contrast, correctly accounts for the intrinsic chemical state of the chromophores and therefore can be used to quantitatively evaluate the data. Simple kinetic modeling (see the SI) suggests that upon X-ray exposure, an intermediate state rapidly builds up to a steady-state level of $\sim 20\%$, characterized by the structural changes shown in Figure 1b. This intermediate, or the starting green-emitting species, infrequently converts to a permanently bleached state (slow phase in the absorbance decay), yielding the structural changes shown in Figure S4. Importantly, the fast buildup of the intermediate, its steady-state level at $\sim 20\%$, and its slow recovery at 100 K in the absence of X-rays altogether imply that the intermediate is not only induced but also efficiently "repaired" to the initial fluorescent state by X-ray irradiation. Such a repair mechanism probably constitutes a general feature of X-ray-induced radiation chemistry in redox-active biological molecules.

To relate our observations to the mechanism of photodamage induced by visible light, an IrisFP crystal was illuminated at 100 K with 488 nm laser light (see the SI). An irreversible loss of absorbance and fluorescence was achieved, although at short illumination times, a transient rise of the 390 nm absorbance band was also noticed (Figures S5 and S6). We attribute this rise to a photoinduced protonation of the chromophore, possibly involved in the photoswitching mechanism of photochromic FPs, as suggested previously.²⁶ Raman data collected on a crystal after prolonged illumination by 488 nm light, while also suggesting some photoinduced protonation of the chromophore (see the discussion in the SI), reveal a major decrease of the band at 1545 cm⁻¹, as in the X-ray case (Figure 2). Therefore, like the X-rays, visible photons primarily affect the C_α=C₅ double bond that is key to the chromophore's optical properties.

Absorption of a visible photon in FPs may induce radical species arising from electron transfer in an excited state of the chromophore (Figure 3). As suggested for organic dyes,^{8,12} we anticipate that because of its long lifetime, the triplet state T₁ is the most likely starting point for reactions driving the IrisFP chromophore to radical states, although singlet states may also contribute.⁹⁻¹¹ Because of the likely involvement of T₁ and competition with other phototransformation pathways (see the SI), accumulation of a radical state is not expected under visible light at the ensemble level, even at cryogenic temperature. In any case, radical formation by X-rays and visible light proceeds a priori by different mechanisms. We postulate that the strongly reducing electrons and oxidizing holes generated by X-ray-induced solvent radiolysis provide an effective

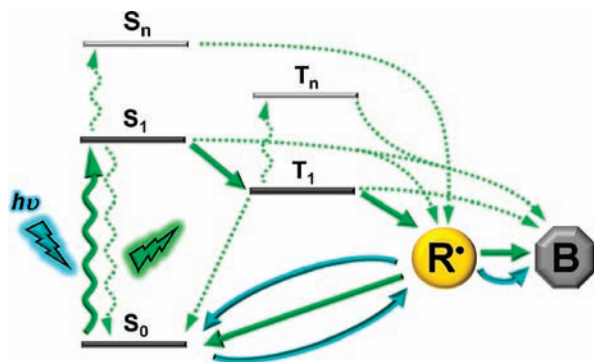


Figure 3. Proposed mechanism for X-ray-induced radical generation in IrisFP and possible photobleaching pathways. Green and blue lines show electron transfer and/or photobleaching pathways induced by visible and X-ray light, respectively. Green dotted lines show other possible pathways not discussed in this article. Notation: R*, radical; B, bleached.

shunt pathway for populating a biologically relevant radical state directly from the ground state.

Our results are in line with recent findings that the fluorescent properties of organics dyes strongly depend on their local redox environment. For example, intermolecular electron transfer from/to reducing/oxidizing agents has been shown to influence the blinking rate of several dyes,^{8,9} offering opportunities to scavenge radical states or to precisely control blinking in superlocalization-based nanoscopy.⁴ The investigation of similar effects in FPs will be of interest in future studies.

Radical states similar to that observed here may also play important roles in FPs. A radical state has been invoked as a putative intermediate in the oxidative green-to-red photoconversion noticed in some GFP members.¹⁷ The mechanism of superoxide release by the red FP KillerRed is also worth mentioning. It can be speculated that electrons extracted from the excited chromophore can be efficiently transferred out of the protein via a chain of water molecules, allowing reduction of O₂ to O₂^{•-}.^{27,28}

In organic dyes, a well-known mechanism of photobleaching is the destruction of the chromophore by reactive oxygen species (ROS), which form when molecular oxygen reacts with the excited chromophore. Some evidence exists that such self-sensitization may not be the dominant cause of photobleaching in FPs,²⁹ as their β -can structure protects the chromophore from the solvent and dissolved O₂. Yet, FPs are typically 1 order of magnitude less resistant to photobleaching than organic dyes. This observation suggests that photobleaching via intramolecular electron transfer might play a comparatively important role in FPs. While the protein matrix tends to protect the chromophore against O₂, it also provides a source of electrons available for redox reactions within the chromophore pocket. In the case of IrisFP (as in GFP¹⁵), charge transfer from Glu212 to the chromophore may occur upon absorption of a visible photon, leaving an unpaired electron on this residue. This biradical state may then relax back to the ground state or occasionally lead to decarboxylation of Glu212, as observed in this work. More photostable variants could perhaps be designed by insertion of sulfur-containing residues exposed to solvent and linked to the chromophore pocket via electron wires.²⁷

Our results underpin the susceptibility of FPs to electron-transfer reactions¹⁷ and reveal the methylene bridge as the Achilles' heel of the chromophore in FPs. Finally, the distortions induced by mild

X-ray irradiation observed here for IrisFP suggest that the chromophore geometry in a number of FPs whose structures have been solved using synchrotron radiation may be slightly overbent.

Acknowledgment. We thank M. Weik and A. Royant for insightful discussions. D.B. acknowledges support by ANR-07-BLAN-0107-01. G.U.N. acknowledges support by the State of Baden-Württemberg and the DFG (Grants CFN, NI 291/9, and SFB 497). S.V. was supported by the CEA.

Supporting Information Available: Materials and methods, kinetic model, solution studies, pH-dependent Raman spectra, phototransformations in IrisFP, data collection statistics, and illustrations. This material is available free of charge via the Internet at <http://pubs.acs.org>.

References

- Wiedenmann, J.; Nienhaus, G. U. *Expert Rev. Proteomics* **2006**, *3*, 361.
- Hell, S. W. *Nat. Methods* **2009**, *6*, 24.
- Dickson, R. M.; Cubitt, A. B.; Tsien, R. Y.; Moerner, W. E. *Nature* **1997**, *388*, 355.
- Vogelsang, J.; Cordes, T.; Forthmann, C.; Steinhauer, C.; Tinnefeld, P. *Proc. Natl. Acad. Sci. U.S.A.* **2009**, *106*, 8107.
- Fölling, J.; Bossi, M.; Bock, H.; Medda, R.; Wurm, C. A.; Hein, B.; Jakobs, S.; Eggeling, C.; Hell, S. W. *Nat. Methods* **2008**, *5*, 943.
- Betzig, E.; Patterson, G. H.; Sougrat, R.; Lindwasser, O. W.; Olenych, S.; Bonifacino, J. S.; Davidson, M. W.; Lippincott-Schwartz, J.; Hess, H. F. *Science* **2006**, *313*, 1642.
- White, J.; Stelzer, E. *Trends Cell Biol.* **1999**, *9*, 61.
- Vogelsang, J.; Kasper, R.; Steinhauer, C.; Person, B.; Heilemann, M.; Sauer, M.; Tinnefeld, P. *Angew. Chem., Int. Ed.* **2008**, *47*, 5465.
- Widengren, J.; Chmyrov, A.; Eggeling, C.; Löfdahl, P. A.; Seidel, C. A. M. *J. Phys. Chem. A* **2007**, *111*, 429.
- Yeow, E. K.; Melnikov, S. M.; Bell, T. D.; De Schryver, F. C.; Hofkens, J. J. *J. Phys. Chem. A* **2006**, *110*, 1726.
- Hoogenboom, J. P.; van Dijk, E. M.; Hernandez, J.; van Hulst, N. F.; Garcia-Parajo, M. F. *Phys. Rev. Lett.* **2005**, *95*, 097401.
- Zondervan, R.; Kulzer, F.; Orlinskii, S. B.; Orrit, M. *J. Phys. Chem. A* **2003**, *107*, 6770.
- Wang, X.; Ren, X.; Kahen, K.; Hahn, M. A.; Rajeswaran, M.; Maccagnano-Zacher, S.; Silcox, J.; Cragg, G. E.; Efros, A. L.; Krauss, T. D. *Nature* **2009**, *459*, 686.
- Shaner, N. C.; Lin, M. Z.; McKeown, M. R.; Steinbach, P. A.; Hazelwood, K. L.; Davidson, M. W.; Tsien, R. Y. *Nat. Methods* **2008**, *5*, 545.
- van Thor, J. J.; Gensch, T.; Hellingwerf, K. J.; Johnson, L. N. *Nat. Struct. Biol.* **2002**, *9*, 37.
- Bell, A. F.; Stoner-Ma, D.; Wachter, R. M.; Tonge, P. J. *J. Am. Chem. Soc.* **2003**, *125*, 6919.
- Bogdanov, A. M.; Mishin, A. S.; Yampolsky, I. V.; Belousov, V. V.; Chudakov, D. M.; Subach, F. V.; Verkhusha, V. V.; Lukyanov, S.; Lukyanov, K. A. *Nat. Chem. Biol.* **2009**, *5*, 459.
- Adam, V.; Lelimosin, M.; Boehme, S.; Desfonds, G.; Nienhaus, K.; Field, M. J.; Wiedenmann, J.; McSweeney, S.; Nienhaus, G. U.; Bourgeois, D. *Proc. Natl. Acad. Sci. U.S.A.* **2008**, *105*, 18343.
- Wiedenmann, J.; Ivanchenko, S.; Oswald, F.; Schmitt, F.; Rucker, C.; Salih, A.; Spindler, K. D.; Nienhaus, G. U. *Proc. Natl. Acad. Sci. U.S.A.* **2004**, *101*, 15905.
- Berglund, G. I.; Carlsson, G. H.; Smith, A. T.; Szoke, H.; Henriksen, A.; Hajdu, J. *Nature* **2002**, *417*, 463.
- Schellenberg, P.; Johnson, E.; Esposito, A. P.; Reid, P. J.; Parson, W. W. *J. Phys. Chem. B* **2001**, *105*, 5316.
- He, X.; Bell, A. F.; Tonge, P. J. *J. Phys. Chem. B* **2002**, *106*, 6056.
- Luin, S.; Voliani, V.; Lanza, G.; Bizzari, R.; Amat, P.; Tozzini, V.; Serresi, M.; Beltram, F. *J. Am. Chem. Soc.* **2009**, *131*, 96.
- Garman, E. F.; Owen, R. L. *Acta Crystallogr., Sect. D: Biol. Crystallogr.* **2006**, *62*, 32.
- McGeehan, J.; Ravelli, R. B.; Murray, J.; Owen, R. L.; Cipriani, F.; McSweeney, S.; Weik, M.; Garman, E. *J. Synchrotron Radiat.* **2009**, *16*, 163.
- Mizuno, H.; Mal, T. K.; Walchli, M.; Kikuchi, A.; Fukano, T.; Ando, R.; Jayakanthan, J.; Taka, J.; Shiro, Y.; Ikura, M.; Miyawaki, A. *Proc. Natl. Acad. Sci. U.S.A.* **2008**, *105*, 9227.
- Carpentier, P.; Violot, S.; Blanchoin, L.; Bourgeois, D. *FEBS Lett.* **2009**, *583*, 2839.
- Pletnev, S.; Gurskaya, N. G.; Pletneva, N. V.; Lukyanov, K. A.; Chudakov, D. M.; Martynov, V. I.; Popov, V. O.; Kovalchuk, M. V.; Wlodawer, A.; Dauter, Z.; Pletnev, V. J. *Biol. Chem.* **2009**, *284*, 32028.
- Swaminathan, R.; Hoang, C. P.; Verkman, A. S. *Biophys. J.* **1997**, *72*, 1900.

JA907296V